High Resolution Cross-Well Imaging of a West Texas Carbonate Reservoir: Part 2. Wavefield Analysis and Tomography

BG1.3

M. Van Schaack, J. M. Harris, Stanford Univ.; J. W. Rector III, Univ. of California, Berkeley (formerly Stanford Univ.); and S. K. Lazaratos, Stanford Univ.*

SUMMARY

We have collected a crosswell seismic dataset of nearly 40,000 traces in a West Texas carbonate oilfield. In this paper we discuss the wavefield analysis and tomographic processing of this survey. Data were collected at 2.5 foot intervals in both the source and receiver wells. The surveyed zone is about 500 feet in extent with the primary target being the approximately 100 foot thick Permian-aged Grayburg formation. The offset between the two wells is nominally 184 feet.

The cylindrical piezoelectric bender source provided ample signal strength and high quality data were collected with a very good signal to noise ratio containing frequencies from 250-2000 Hertz. These data contain a rich variety of seismic modes. Among the easily identifiable modes are; direct p-wave, direct s-wave, reflected p-wave, reflected s-wave, p-s conversions, s-p conversions, head waves, and of course, tube waves. Despite the intimidating complexity of the seismic records many wave modes (except tube waves) are simulated very effectively. A radial point force and the radial stress component are used to model the cylindrical piezoelectric bender source and the hydrophones respectively. A blocked sonic well log is used as a 1-D velocity model.

The quality of the signal in combination with high density coverage has made possible an excellent velocity tomogram. Information gained through the wavefield modelling was used in developing a suitable processing scheme for the traveltime tomography. The tomogram converges with a traveltime residual of less than 100us and ties very well with the velocities of the sonic well logs in the vicinity of the borehole. The resolution is good and a response from a number of 10-20 foot thick beds can be seen in a comparison of tomogram velocities and well logs.

INTRODUCTION

Traveltime tomography has been in use as a tool for imaging velocity structure between wells for a number of years now. Great strides have been made in the development of inversion algorithms as is evident by the great number of techniques now being used. Despite this, many tomographic velocity images yield disappointing results, especially when compared to well log velocities and known geologic structure. The ability of traveltime tomography to accurately image velocities is adversely affected by a number of factors. Included in these is limited view, limited spectral bandwidth, dispersion, attenuation, measurement errors, and velocity anisotropy. Some of these factors are, unfortunately, a result of the experimental setup itself while others, such as velocity anisotropy, could be handled by more sophisticated inversion algorithms. Work being done to incorporate anisotropy into the inversion process has shown promise (Michelena, 1992).

Many times though, differences between well log and tomogram velocities, and/or structures within the tomogram, are inexplicable in light of the known geology. This may often be due to a processing scheme not well suited to the data to be inverted. In many cases the inversion process can be drastically improved through the use of synthetic modelling to guide the picking and processing of the field data.

In this paper we use a simplistic source, receiver, and geologic model to identify the many wave modes observed in the field data. Despite the absence of source and receiver boreholes in our wavefield simulations we find a remarkable similarity between our field data and the simulated data. The model developed in this analysis is used as the basis for creating a synthetic dataset. A processing flow developed to optimize the inversion of the synthetic data is then used to optimize processing parameters for the inversion of the field data. The site and acquisition of the field survey are described in detail in Harris, et al. (1992). We find after processing that we achieve a very good tie with the well logs and that a number of thin beds are imaged by the tomography.

SIMULATIONS

The simulations were run using Sierra Geophysics' viscoelastic seismic profiling program VESPA (Apsel, 1979). The tie of synthetic data to field data using a 1-D geologic model confirms interpretation of the well logs which suggest a predominantly flat geology over the surveyed zone. There is a mild dip in structure in the deeper section of the surveyed area. This is supported both by the logs and by reflection imaging done using this crosswell dataset (Lazaratos et al, 1992).

We use a radial horizontal point force to model our source. We feel this is justified for several reasons. One is the relative size of the shortest wavelength compared to the source length is about 5 to 1. Also, in this survey, the outside diameter of the source was only about 1/4" less than the inside diameter of the casing. This tight tolerance should maximize the energy introduced into the formation perpendicular to the borehole axis. We feel this explains the low relative amplitudes of the tube waves to the direct and reflected arrivals.

To model our hydrophone response we extract the radial stress component of the wavefield. In VESPA the coordinate system is cylindrical so the radial stress component is equal the horizontal stress. The interaction between the seismic wavefield and the receiver borehole is complicated with conversions of shear to compressional waves being the most difficult to predict. As our hydrophone is basically a pressure transducer it seems reasonable that the pressure inside a borehole would be best approximated by the stress perpendicular to the axis of the borehole.

The geologic model was created using blocked data from the sonic shear and compressional well logs. A shear sonic log was run only in the receiver well so the blocked logs from this well were used for our 1-D model. The simulations shown in this paper were created using a geologic model with 200 distinct layers ranging in thickness from 6 inches to several feet. Figure 1 shows a schematic view of the simulation geometry. Figure 2 shows a typical receiver gather from our measured dataset.

The results of our simulations compare well with the raw field data. All of the obvious modes seen in the synthetic seismogram can be found in the field data (figures 3-6). Even exotic converted wave modes predicted by our simulations are seen. The degree to which our synthetic and field data agree suggest that the borehole effect is not very large for the piezoelectric bender source under the conditions it was run. Certainly the high velocities eliminated the possibility of certain modes, such as the Mach wave (Meredith, 1990). Also, the simulations support log and local geologic information which suggest a predominantly flat geologic structure with little velocity anisotropy.

The lack of any unexplainable wave modes of significant amplitude is certainly encouraging with respect to efforts in our group directed toward reflection processing and imaging. We can develop processing techniques confident that our subtle manipulations are not overwhelmed by unaccounted for large amplitude wave modes. Wavefield processing and reflection imaging of this crosswell dataset can be found in Lazaratos et al. (1992), and Rector et al. (1992).

TOMOGRAPHY

Following the data editing and geometry definition, first break p-wave traveltimes were picked from the field data. Although hand picking nearly 40,000 traces may seem a daunting task, first pass picking was accomplished in only one 3 hour session. The general philosophy for this first cut picking was to pick on first arriving energy without trying to decipher headwaves from direct arrivals.

Traveltime picks were inverted using the STRINGS inversion code (Harris et al., 1990). This algorithm is an iterative method. Due to the size of the dataset, algebraic reconstruction techniques are powerful and effective, and in fact crucial, in inversion of the data with the computing power at our disposal.

Traveltimes calculated through a starting model are compared to measured traveltimes. The differences between these two traveltimes are used to calculate a correction to the starting model. The model is then updated and used as the starting model for the next iteration. This process is carried on through subsequent iterations until the residual reaches an acceptable level.

Figure 7 shows the results of a tomogram calculated using a homogeneous starting model. This was done along with using the unbiased first break traveltimes to minimize the effect of any preconceptions on this first tomogram. The first several iterations of our inversion were designed to calculate a 1-D solution for the data. This 1-D model was then used to start our 2-D inversion. A total of 7 iterations was used for this inversion by which time the average absolute value of the traveltime residual had stabilized to less than 100us (1/2 a sample interval).

The flat geologic structure of the surveyed zone is seen very clearly in the tomogram and ties well with the structure suggested by the well logs. Particularly remarkable is the tie between the sonic well logs and the tomogram velocities at the well (figures 8 & 9). Not only are the average velocity values accurately calculated but we can see the effect of several beds as thin as 10-20 feet in the tomogram. Although these beds are not in any real sense 'resolved' the results suggest that a more careful choice in the starting model and model based picking might further bring out these subtle features. It should be noted that resolution of beds as thin as the shortest wavelength, which is approximately 10 feet in our survey, approaches the theoretical limits of what is possible with traveltime tomography.

CONCLUSIONS

The results of our work show the importance of careful experiment design and data collection to traveltime tomography. Model based analysis of the data is invaluable in guiding and developing a suitable processing scheme for accurate tomographic inversion. Since the design and execution of the tomographic survey is so strongly affected by the geology of the surveyed area proper model based analysis is essential in ensuring the best results possible.

ACKNOWLEDGEMENTS

The authors are grateful to the Gas Research Institute for support in this research and to Chevron Oil Field Research Company for providing the field site and co-sponsoring this study at Stanford.

REFERENCES

Apsel, R.J., 1979, Dynamic Green's Functions for Layered Media and Application to Boundary-Value Problems, Ph.D. Thesis, University of California at San Diego.

Harris, J.M., Lazaratos, S.K., Michelena, R.J., 1990, Tomographic String Inversion, STP volume1, paper B.

Harris, J.M., Nolen-Hoeksema, R., Rector, J.W., Van Schaack, M.A., Lazaratos, S.K., 1992, High Resolution Crosswell Imaging of a West Texas Carbonate Reservoir: Part 1 - Project Overview: presented at the 62nd Ann. Internat. Mtg., Soc. Expl. Geophys.

Lazaratos, S.K., Rector, J.W., Harris, J.M., Van Schaack, M.A., 1992, High Resolution Crosswell Imaging of a West Texas Carbonate Reservoir: Part 4 - Reflection Imaging: presented at the 62nd Ann. Internat. Mtg., Soc. Expl. Geophys.

Meredith, J.A., 1990, Numerical and Analytical Modelling of Downhole Seismic Sources: The Near and Far Field: Ph.D. Thesis, Massachusetts Institute of Technology

Michelena, R.J., 1992, Traveltime Tomography in Azimuthally Anisotropic Media: presented at the 62nd Ann. Internat. Mtg., Soc. Expl. Geophys.

Rector, J.W., Lazaratos, S.K., Harris, J.M., Van Schaack, M.A., 1992, High Resolution Crosswell Imaging of a West Texas Carbonate Reservoir: Part 3 - Wavefield Separation: presented at the 62nd Ann. Internat. Mtg., Soc. Expl. Geophys.

Figure 1

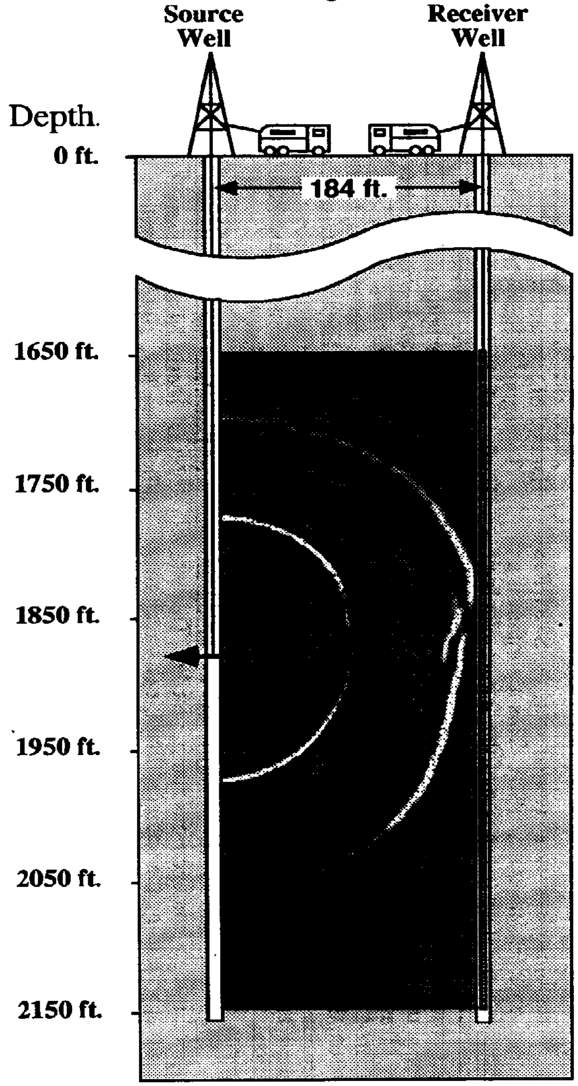

Figure 1) Schematic of crosswell synthetic setup. The source is modelled by a horizontal radial point force. The receivers are modelled by radial (horizontal) stress. The waveform shown is a snapshot of the radial stress field at 10ms. for a shot depth of 1880 feet.
Figure 2) Unprocessed common receiver gather for a receiver depth of 1880 feet.

Figure 2

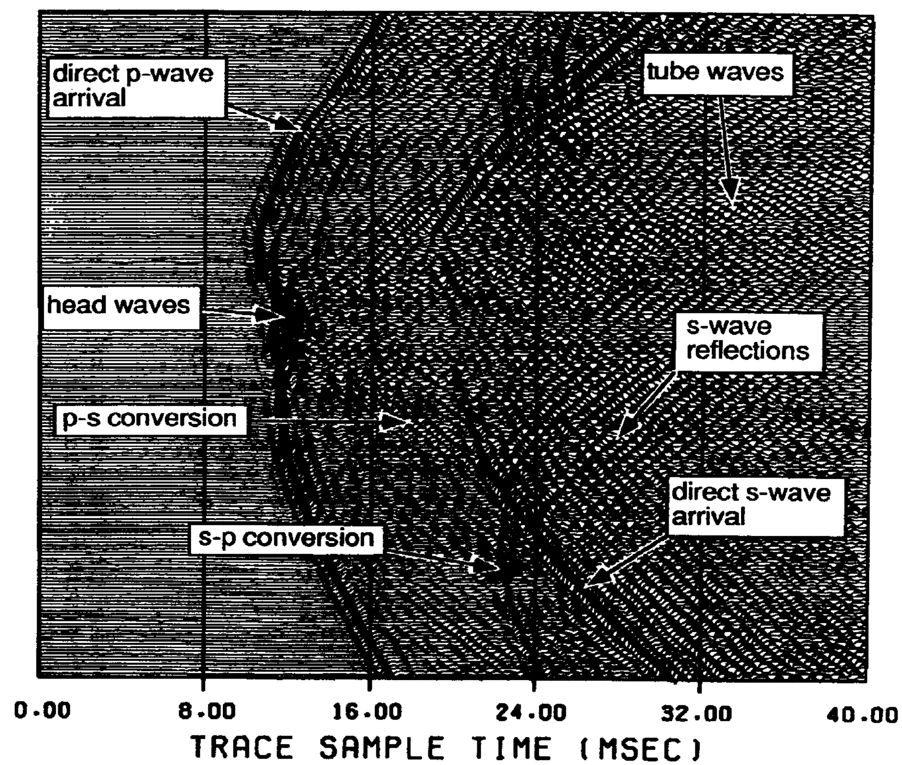

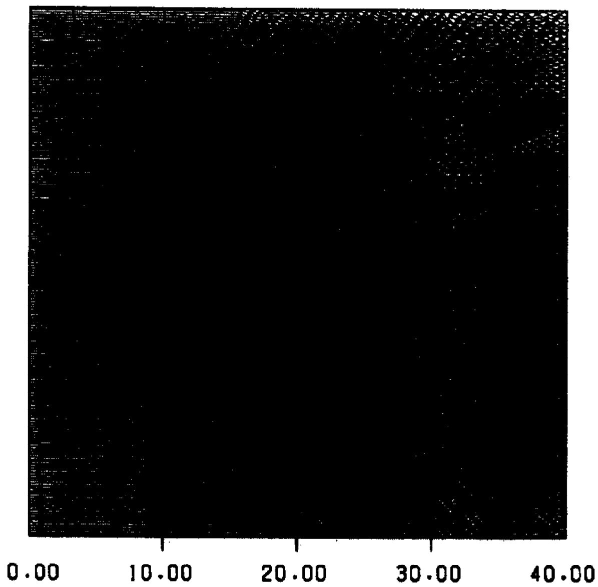

Figure 3) Field data. The above seismic record is an unprocessed common receiver gather. Shot spacing for this record is 2.5 feet for a total coverage of 500 feet. Receiver depth is approximately 1880 feet (see figure 1). Time is in milliseconds.

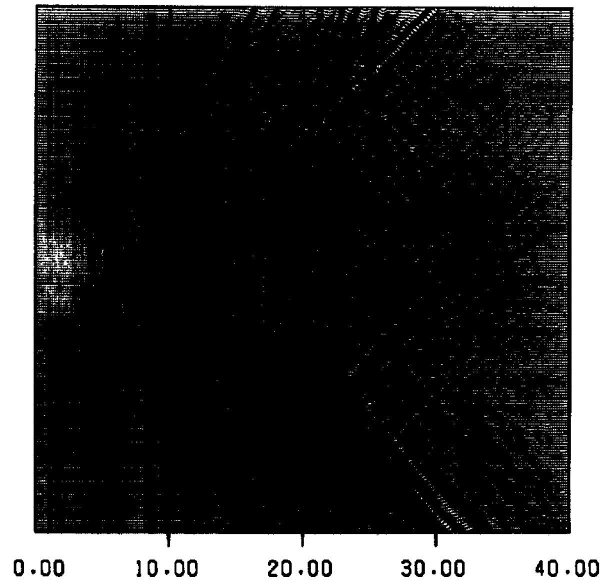

Figure 4) Synthetic data. The above is a full wave simulation. The source is modelled by a radial point force and the hydrophones by radial (horizontal) stress. The sonic well logs from the field survey receiver well, blocked into 200 layers, were used to create the velocity model. Time is in milliseconds.

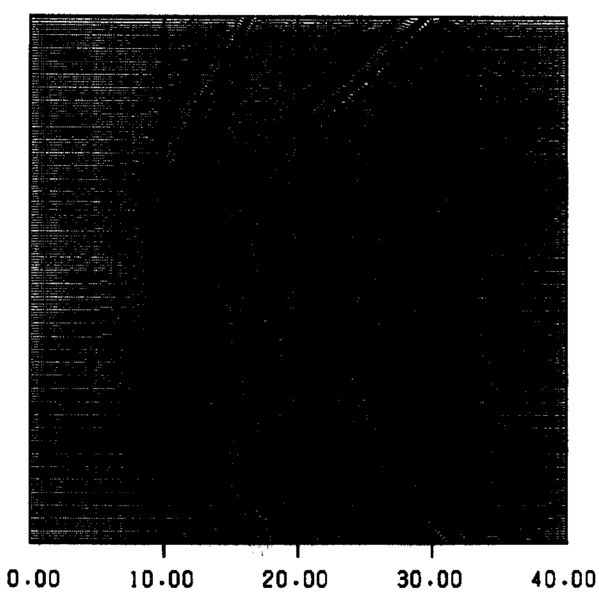

Figure 5) Synthetic data. This simulation is the same as in figure 4 except with suppressed multiples and conversions. The only arrivals are direct p and s wave and primary p and s wave reflections. Time is in milliseconds.

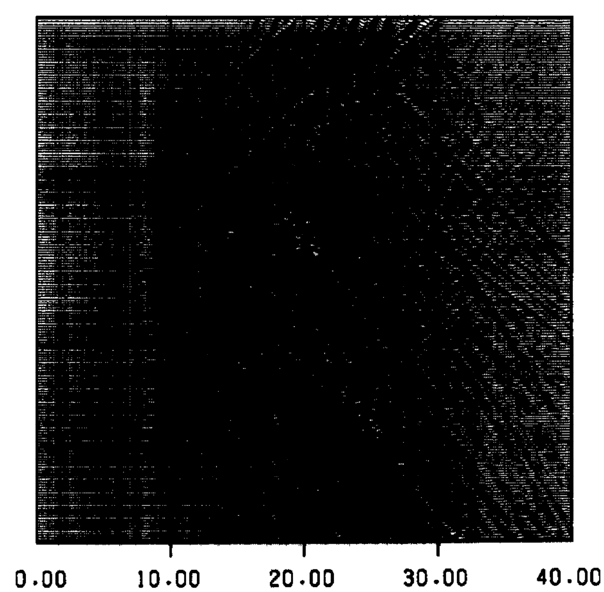

Figure 6) Synthetic data. This simulation is also the same as figure 4 except only p and s wave conversions are shown. The gain display has been increased to accentuate the waveforms. Time is in milliseconds.

Figure 7

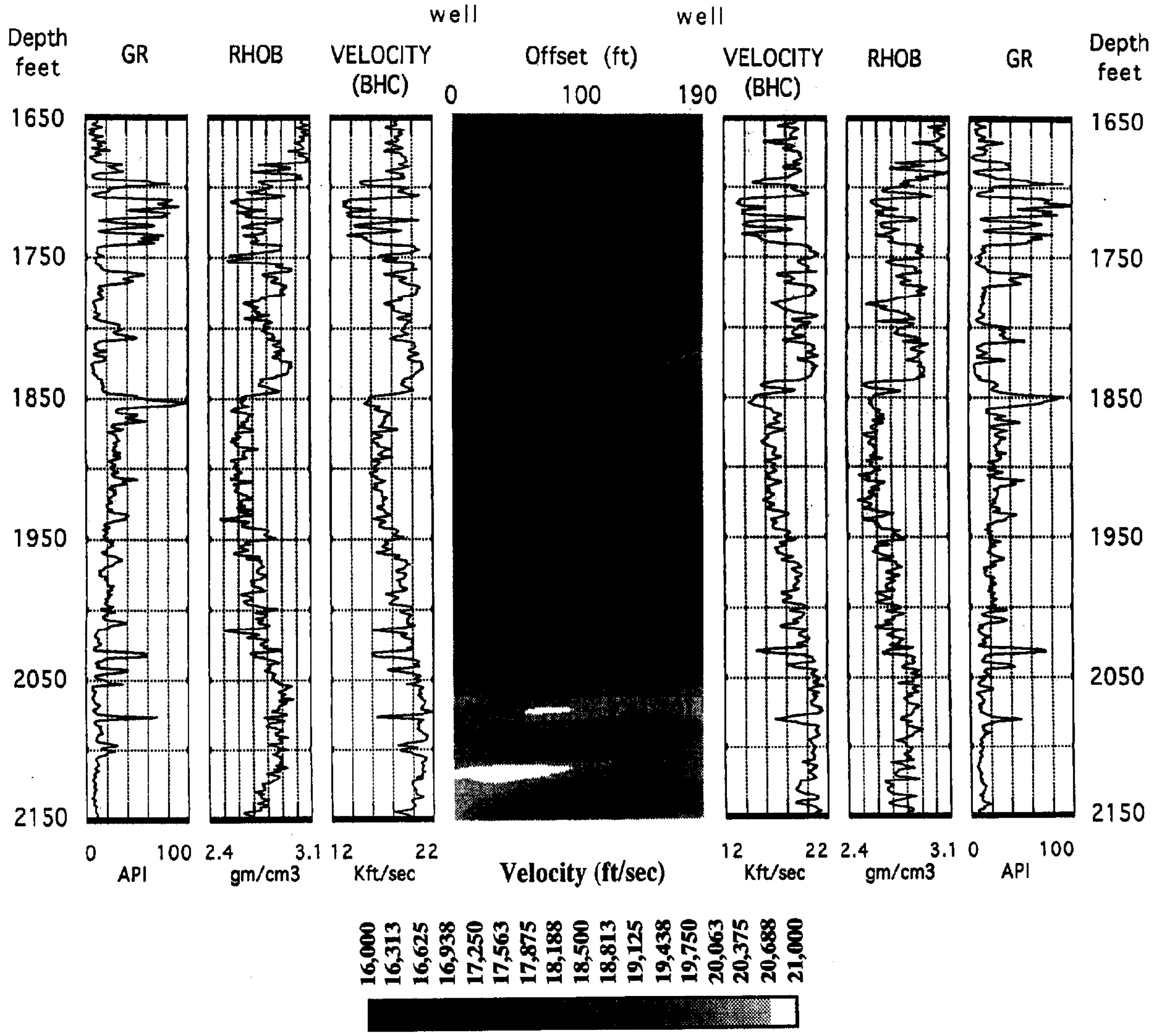

Figure 8

Receiver Well

Tomogram Velocity vs Well Log Velocity

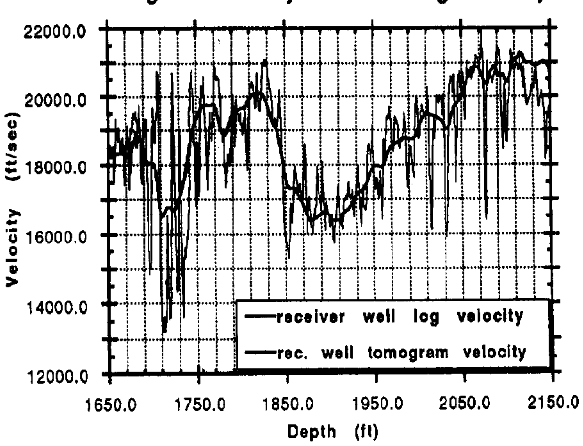

Figure 9

Source Well

Tomogram Velocity vs Well Log Velocity

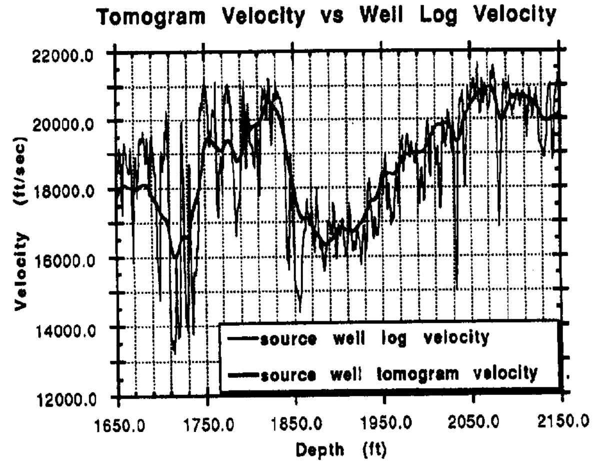

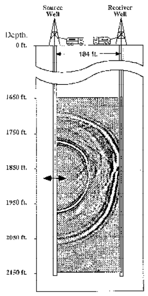
Source Well
Receiver Well
Depth.
0 ft.
184 ft.
1650 ft.
1750 ft.
1850 ft.
1950 ft.
2050 ft.
2150 ft.

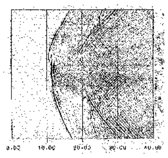
10.00
20.00